



This is a repository copy of *Cold-season methane fluxes simulated by GCP-CH4 models*.

White Rose Research Online URL for this paper:

<https://eprints.whiterose.ac.uk/201839/>

Version: Published Version

---

**Article:**

Ito, A. [orcid.org/0000-0001-5265-0791](https://orcid.org/0000-0001-5265-0791), Li, T. [orcid.org/0000-0002-6338-2769](https://orcid.org/0000-0002-6338-2769), Qin, Z. [orcid.org/0000-0001-9414-4854](https://orcid.org/0000-0001-9414-4854) et al. (21 more authors) (2023) Cold-season methane fluxes simulated by GCP-CH4 models. *Geophysical Research Letters*, 50 (14). ISSN 0094-8276

<https://doi.org/10.1029/2023gl103037>

---

**Reuse**

This article is distributed under the terms of the Creative Commons Attribution (CC BY) licence. This licence allows you to distribute, remix, tweak, and build upon the work, even commercially, as long as you credit the authors for the original work. More information and the full terms of the licence here:

<https://creativecommons.org/licenses/>

**Takedown**

If you consider content in White Rose Research Online to be in breach of UK law, please notify us by emailing [eprints@whiterose.ac.uk](mailto:eprints@whiterose.ac.uk) including the URL of the record and the reason for the withdrawal request.



[eprints@whiterose.ac.uk](mailto:eprints@whiterose.ac.uk)  
<https://eprints.whiterose.ac.uk/>

# Geophysical Research Letters<sup>®</sup>



## RESEARCH LETTER

10.1029/2023GL103037

### Key Points:

- Cold-season methane (CH<sub>4</sub>) emissions simulated by 16 Global Carbon Project-CH<sub>4</sub> wetland models were analyzed
- Most models underestimate the cold-season emissions in comparison with observational data
- Further model improvement by including cold-season processes is required to reduce the model bias and uncertainty

### Supporting Information:

Supporting Information may be found in the online version of this article.

### Correspondence to:

A. Ito,  
[itoh@nies.go.jp](mailto:itoh@nies.go.jp)

### Citation:




















Ito, A., Li, T., Qin, Z., Melton, J. R., Tian, H., Kleinen, T., et al. (2023). Cold-season methane fluxes simulated by GCP-CH<sub>4</sub> models. *Geophysical Research Letters*, 50, e2023GL103037. <https://doi.org/10.1029/2023GL103037>

Received 1 FEB 2023  
Accepted 16 JUN 2023

### Author Contributions:

**Conceptualization:** A. Ito  
**Formal analysis:** A. Ito  
**Investigation:** A. Ito  
**Project Administration:** B. Poulter  
**Resources:** T. Li, Z. Qin, J. R. Melton, H. Tian, T. Kleinen, W. Zhang, Z. Zhang, F. Joos, P. Ciais, P. O. Hopcroft, D. J. Beerling, X. Liu, Q. Zhuang, Q. Zhu, C. Peng, K.-Y. Chang, E. Fluet-Chouinard, G. McNicol, P. Patra, B. Poulter, S. Sitch, W. Riley, Q. Zhu  
**Validation:** A. Ito  
**Visualization:** A. Ito  
**Writing – original draft:** A. Ito

## Cold-Season Methane Fluxes Simulated by GCP-CH<sub>4</sub> Models

A. Ito<sup>1,2,3,4</sup> , T. Li<sup>5,6</sup> , Z. Qin<sup>6,7</sup> , J. R. Melton<sup>8</sup>, H. Tian<sup>9</sup>, T. Kleinen<sup>10</sup> , W. Zhang<sup>11</sup> , Z. Zhang<sup>12</sup>, F. Joos<sup>13</sup> , P. Ciais<sup>14</sup> , P. O. Hopcroft<sup>15</sup> , D. J. Beerling<sup>16</sup>, X. Liu<sup>17</sup> , Q. Zhuang<sup>17</sup> , Q. Zhu<sup>18</sup>, C. Peng<sup>19</sup> , K.-Y. Chang<sup>20</sup> , E. Fluet-Chouinard<sup>21</sup> , G. McNicol<sup>22</sup> , P. Patra<sup>2</sup> , B. Poulter<sup>23</sup> , S. Sitch<sup>24</sup> , W. Riley<sup>20</sup> , and Q. Zhu<sup>20</sup> 

<sup>1</sup>National Institute for Environmental Studies, Tsukuba, Japan, <sup>2</sup>Japan Agency for Marine-Earth Science and Technology, Yokohama, Japan, <sup>3</sup>Tohoku University, Sendai, Japan, <sup>4</sup>Nagoya University, Nagoya, Japan, <sup>5</sup>Institute of Atmospheric Physics, Chinese Academy of Sciences, Beijing, China, <sup>6</sup>Southern Marine Science and Engineering Guangdong Laboratory (Zhuhui), Zhuhai, China, <sup>7</sup>Sun Yat-sen University, Zhuhai, China, <sup>8</sup>Climate Research Division, Environment and Climate Change Canada, Victoria, BC, Canada, <sup>9</sup>Boston College, Schiller Institute for Integrated Science and Society, Chestnut Hill, MA, USA, <sup>10</sup>Max Planck Institute for Meteorology, Hamburg, Germany, <sup>11</sup>Lund University, Lund, Sweden, <sup>12</sup>University of Maryland, College Park, MD, USA, <sup>13</sup>University of Bern, Bern, Switzerland, <sup>14</sup>Laboratoire des Sciences du Climat et de l'Environnement, Gif sur Yvette, France, <sup>15</sup>University of Birmingham, Birmingham, UK, <sup>16</sup>University of Sheffield, Sheffield, UK, <sup>17</sup>Purdue University, West Lafayette, IN, USA, <sup>18</sup>Hohai University, Nanjing, China, <sup>19</sup>University of Quebec at Montreal, Montreal, QC, Canada, <sup>20</sup>Lawrence Berkeley National Laboratory, Berkeley, CA, USA, <sup>21</sup>ETH Zurich, Zurich, Switzerland, <sup>22</sup>University of Illinois Chicago, Chicago, IL, USA, <sup>23</sup>NASA Goddard Space Flight Center, Greenbelt, MD, USA, <sup>24</sup>University of Exeter, Exeter, UK

**Abstract** Cold-season methane (CH<sub>4</sub>) emissions may be poorly constrained in wetland models. We examined cold-season CH<sub>4</sub> emissions simulated by 16 models participating in the Global Carbon Project model intercomparison and analyzed temporal and spatial patterns in simulation results using prescribed inundation data for 2000–2020. Estimated annual CH<sub>4</sub> emissions from northern (>60°N) wetlands averaged  $10.0 \pm 5.5$  Tg CH<sub>4</sub> yr<sup>-1</sup>. While summer CH<sub>4</sub> emissions were well simulated compared to in-situ flux measurement observations, the models underestimated CH<sub>4</sub> during September to May relative to annual total ( $27 \pm 9\%$ , compared to 45% in observations) and substantially in the months with subzero air temperatures ( $5 \pm 5\%$ , compared to 27% in observations). Because of winter warming, nevertheless, the contribution of cold-season emissions was simulated to increase at  $0.4 \pm 0.8\%$  decade<sup>-1</sup>. Different parameterizations of processes, for example, freezing–thawing and snow insulation, caused conspicuous variability among models, implying the necessity of model refinement.

**Plain Language Summary** Wetlands in the northern high latitudes are a major source of methane (CH<sub>4</sub>) to the atmosphere, mainly during the warm season. Previously, models have assumed that cold-season CH<sub>4</sub> emissions are low, but recent observations suggest high-latitude wetlands can be substantial sources even in winter. We compared CH<sub>4</sub> emissions simulated by 16 state-of-the-art wetland models, participating in a model intercomparison project with a focus on the cold-season in northern wetlands. The model simulations indicated that nearly one third of annual emissions were simulated to occur from September to May, and CH<sub>4</sub> emissions to the atmosphere were not negligible even under freezing air temperatures, although the results differed greatly among the models. However, field studies suggest cold-season emissions account for an even larger fraction of annual emissions. These results highlight the contribution of cold-season emissions to the annual CH<sub>4</sub> budget, which future climatic warming is expected to affect severely, and they also show that simulations of cold-season CH<sub>4</sub> emissions from wetlands need to be improved.

## 1. Introduction

Methane (CH<sub>4</sub>) is a potent, short-lived greenhouse gas that contributes to anthropogenic climatic change and air pollution (Dlugokencky et al., 2011; Nisbet et al., 2019). Because of its relatively short lifetime in the atmosphere (~9 years: IPCC, 2021), understanding CH<sub>4</sub> emissions is important for mitigation of near-future climatic change, as highlighted by the recent Global Methane Pledge (Global Methane Pledge, 2021). The global methane budget remains uncertain, however, because methane is produced and consumed via multiple spatially and temporally variable pathways. Global CH<sub>4</sub> syntheses by the Global Carbon Project (GCP) (e.g., Jackson et al., 2020; Saunio

© 2023. The Authors.

This is an open access article under the terms of the [Creative Commons Attribution License](https://creativecommons.org/licenses/by/4.0/), which permits use, distribution and reproduction in any medium, provided the original work is properly cited.

**Writing – review & editing:** T. Li, Z. Qin, J. R. Melton, H. Tian, T. Kleinen, W. Zhang, Z. Zhang, F. Joos, P. Ciais, P. O. Hopcroft, D. J. Beerling, X. Liu, Q. Zhuang, C. Peng, K.-Y. Chang, E. Fluet-Chouinard, G. McNicol, P. Patra, B. Poulter, S. Sitch, Q. Zhu

et al., 2020) using contemporary atmospheric and ground observations and model-based analyses provide the most comprehensive estimate of methane sources and sinks to date.

Wetlands are the largest natural source of CH<sub>4</sub> to the atmosphere, contributing approximately 150 Tg CH<sub>4</sub> yr<sup>-1</sup> globally (Saunois et al., 2020). Natural wetlands, ranging from tropical swamps to northern lowlands (e.g., Hudson Bay and West Siberia) and tundra, are distributed worldwide. CH<sub>4</sub> is mainly produced by microbial processes in wet soils, and its efflux is highly sensitive to environmental conditions such as temperature, water-table position, and substrate availability (Le Mer & Roger, 2001; Xu et al., 2016). These methanogenic processes and their environmental sensitivity are regulated in a complex manner, which creates a challenge for biogeochemical models to reproduce observed CH<sub>4</sub> emissions (Melton et al., 2013; Poulter et al., 2017). In terms of the global CH<sub>4</sub> budget and climatic change, the northern wetlands and permafrost are particularly important, both because of their vast area (about 3.5 × 10<sup>6</sup> km<sup>2</sup>; Bubier & Moore, 1994), huge carbon stock (1,035 ± 150 Pg C; Hugelius et al., 2014), and faster climatic warming rates than the global average (IPCC, 2021). It is critical, therefore, to reduce model uncertainties associated with different model structures, parameterizations, and input data to better constrain the global CH<sub>4</sub> budget and to allow more reliable future projections of wetland emissions.

A growing number of in situ studies have revealed that the behavior of wetland CH<sub>4</sub> emissions at temperatures near or below freezing is both important and complex. Observations show that CH<sub>4</sub> emissions in the cold (non-summer) season (September to May) account for more than 50% of the annual CH<sub>4</sub> flux from Arctic tundra (Howard et al., 2020; Röbger et al., 2022; Zona et al., 2016). Observational studies also indicate that cold-season emission rates vary considerably; rates are high at the onset of freezing and thawing (Bao et al., 2021; Elberling et al., 2008; Mastepanov et al., 2008; Pirk et al., 2016) as well as during the “zero-curtain” period (when soil temperatures are near 0°C; Arndt et al., 2019). Particularly drastic variations in CH<sub>4</sub> fluxes such as burst emissions have been observed at soil temperatures close to 0°C (e.g., Mastepanov et al., 2008). Such findings have been made possible by recent technical advancements in measuring gas fluxes during the cold-season, but winter flux data are still sparse and insufficient (e.g., Pallandt et al., 2022). Recently, regional data have been provided by satellite remote sensing of atmospheric CH<sub>4</sub> (e.g., Qu et al., 2021), but it is difficult to apply this technique during the cold-season at high latitudes because of the low solar angle.

There remain large uncertainties in the estimation of wetland CH<sub>4</sub> emissions even by present state-of-the-art models. Model intercomparison studies (e.g., Bohn et al., 2015; Chang et al., 2023) imply that the wetland models can simulate different magnitudes of fluxes though using standardized input data and protocols. The uncertainty, likely coming from differences in model structure and parameterization of CH<sub>4</sub> processes such as methanotrophic production and transports, would be evident for cold-season fluxes. Using flux measurement and model-derived datasets (WETCHIMP and WetCHARTs), Treat et al. (2018) concluded that wetland models have underestimated cold-season CH<sub>4</sub> emissions. The models have estimated the cold-season flux to be negligible because microbial CH<sub>4</sub> production and consumption are strongly inhibited in cold and frozen soils (Bartlett & Harriss, 1993; Christensen, 1993; Ito, 2019). In addition, soil-freezing and snow cover are likely to reduce soil gas diffusivity by disrupting major CH<sub>4</sub> transport pathways (ebullition and plant aerenchyma), at least temporarily, while vegetation dormancy reduces the belowground substrate supply (Olefeldt et al., 2013; Treat et al., 2018).

In this study, we analyze cold-season CH<sub>4</sub> fluxes from northern wetlands as simulated by 16 terrestrial biogeochemical models that participated in the GCP model intercomparison (Poulter et al., 2017, updated in 2022). Using different definitions for the cold-season, we compare CH<sub>4</sub> emissions simulated by multiple models and examine the apparent temperature dependence of the CH<sub>4</sub> flux at freezing and thawing temperatures. Then, on the basis of this diagnosis of current modeling capabilities, we describe current challenges facing the modeling of cold-season CH<sub>4</sub> fluxes and propose key areas for future research.

## 2. Methods

### 2.1. Wetland Models and Simulations

The wetland models used in this study are summarized in Table 1. In general, the models incorporate hydrological and biogeochemical schemes that simulate the water and carbon dynamics of wetlands to enable them to estimate wetland CH<sub>4</sub> fluxes (Table S1 in Supporting Information S1). Although several models can estimate wetland extent dynamically, in this study, the results of simulations based on prescribed wetland extent (i.e., diagnostic experiments) were used to focus on biogeochemical processes.

**Table 1**  
*The 16 Wetland Models*

Model	Rows × columns	References
CH4MOD <sub>wetland</sub>	360 × 720	Li et al. (2016, 2020)
CLASSIC	53 × 128	Arora et al. (2018)
DLEM	360 × 720	Tian et al. (2010)
ELM-ECA	360 × 720	Riley et al. (2011)
ISAM	360 × 720	Shu et al. (2020)
JSBACH	96 × 192	Kleinen et al. (2020)
JULES	360 × 720	Clark et al. (2011)
LPI-GUESS	360 × 720	Wania et al. (2010), McGuire et al. (2012), Spahni et al. (2013)
LPI-MPI	360 × 720	Kleinen et al. (2012)
LPI-wsl	360 × 720	Zhang et al. (2016)
LPX-Bern	360 × 720	Spahni et al. (2011)
ORCHIDEE	180 × 360	Ringeval et al. (2010)
SDGVM	360 × 720	Singarayer et al. (2011)
TEM-MDM	360 × 720	Liu et al. (2020)
TRIPLEX-GHG	582 × 1,440	Zhu et al. (2014)
VISIT	360 × 720	Ito and Inatomi (2012)

The experimental protocol was updated from WETCHIMP (Melton et al., 2013), such that each model is required to conduct prognostic and diagnostic runs using two climate forcing data. The prognostic run uses model-estimated wetland extent, while the diagnostic run uses the remotely sensed monthly wetland inundation data from the WAD2M data set (Zhang et al., 2021). The protocol requires the use of two climate datasets (surface air temperature, humidity, pressure, precipitation, wind speed, and incoming shortwave and longwave radiation): the Climate Research Unit 4.06 (Harris et al., 2020) and the Global Soil Wetness Project Phase three datasets. This study chose the former because it covers the longest period of the two, and we did not find a substantial difference between the results using the two climate datasets. In this study, we analyzed simulated monthly mean  $0.5^\circ \times 0.5^\circ$  gridded  $\text{CH}_4$  flux data ( $\text{kg CH}_4 \text{ m}^{-2} \text{ s}^{-1}$ ). For composite model mapping, data of several models (Table 1) were regridded using the “remapbil” function from Climate Data Operators (<https://code.mpimet.mpg.de/projects/cdo/>).

## 2.2. Observational $\text{CH}_4$ Datasets

Observed  $\text{CH}_4$  flux data were used only for evaluation of the simulation results. The field  $\text{CH}_4$  flux observations were made by eddy covariance method, which generally have a local-scale footprint (on the order of  $\text{m}^2$  to  $\text{km}^2$ ). Therefore, we adopted the data set of Peltola et al. (2019), which comprised  $\text{CH}_4$  flux data observed by the eddy covariance method at 25 northern wetlands sites scaled up with a machine learning algorithm to generate a continuous field for the land area north of  $45^\circ\text{N}$  at a spatial resolution comparable to that of the wetland models. This data set provides the monthly  $\text{CH}_4$  fluxes during 2013–2014 for three different base wetland maps; we used the results for the Global Lakes and Wetlands Data set base map (Lehner & Döll, 2004). Additionally, to examine in situ  $\text{CH}_4$  fluxes closely, we used the FLUXNET- $\text{CH}_4$  version 1.0 data set (Delwiche et al., 2021; Knox et al., 2019), which contains observational data from freshwater wetlands worldwide, including 16 northern wetland sites (wet tundra [inundated temporarily], bogs [ombrotrophic], and fens [minerotrophic]). Note that many sites provide data for only the summer growing season, which may affect the quality of the flux upscaling. For the sites used by Peltola et al. (2019), we found that 15 sites provided data for periods longer than 12 months and at least seven sites (FI-Sii, FI-Si2, US-Los, US-Bes, US-Ivo, Ru-Ch2, and SE-Deg) provided many  $\text{CH}_4$  flux data at subzero air temperature conditions.

## 2.3. Analyses

There are several definitions of “cold-season,” affecting the interpretation of observational data (Rafat et al., 2022). This study considered three definitions of the cold-season: (a) the subzero monthly-mean air

temperature period irrespective of calendar month, determined at each grid; (b) the non-summer months approximating the non-growing period in northern high latitudes, from September to May (the same months as those used by Zona et al., 2016); and (c) the midwinter months from December to February, when soils are assumed to be entirely frozen. The second and third ones are defined simply by calendar and then can contain warm spells. In contrast, cold-season defined by the first one focuses on cold periods only but can vary year-by-year. When focusing on the “zero-curtain” period, we extracted data at air temperatures between  $-5^{\circ}$  and  $5^{\circ}\text{C}$  in spring (March to May) and autumn (September to November), assuming that soil temperature is at around  $0^{\circ}\text{C}$ . Note that this study used air temperature for analyses, primarily due to data availability of model-simulated soil temperatures, but it has several justifications. Rafat et al. (2022) showed that air temperature well represented the non-growing season of  $\text{CO}_2$  emissions, and Knox et al. (2019) showed that the responsiveness of the observed  $\text{CH}_4$  flux to air temperature ( $R^2 = 0.65$ ) is comparable to its responsiveness to soil temperature ( $R^2 = 0.66$ ). Simulated wetland  $\text{CH}_4$  emissions by the models were split into two regions: arctic to boreal ( $60^{\circ}$ – $90^{\circ}\text{N}$ ) and arctic to cool-temperate ( $45^{\circ}$ – $90^{\circ}\text{N}$ ) regions. These regions were examined for their seasonal and interannual variability, spatial distribution, and relationship with temperature, especially around the freezing point. The temperature–emission relationship is useful for clarifying model-specific behavior, but a large inter-model discrepancy in the flux magnitude can obscure individual model characteristics. Therefore, we used standardized monthly  $\text{CH}_4$  fluxes (= monthly flux/annual flux) in each grid cell to scale the simulated flux magnitudes from the different models.

### 3. Results and Discussion

#### 3.1. Model-Mean Annual Emissions

The 16 wetland models simulated annual  $\text{CH}_4$  emissions during 2000–2020 from wetlands of  $60^{\circ}$ – $90^{\circ}\text{N}$  to be  $10.0 \pm 5.5 \text{ Tg CH}_4 \text{ yr}^{-1}$  and those of  $45^{\circ}$ – $90^{\circ}\text{N}$  as  $26.7 \pm 10.1 \text{ Tg CH}_4 \text{ yr}^{-1}$  (mean across models  $\pm$  standard deviation). These values, which account for 6% and 16%, respectively, of the global total wetland emissions simulated by the models, are slightly lower than the corresponding upscaled flux data (Table S2 in Supporting Information S1). Particularly strong and spatially extensive  $\text{CH}_4$  sources were located in the West Siberia and the Hudson Bay Lowlands, where land grids were dominated by wetlands including wet tundra (Figure S1 in Supporting Information S1).

#### 3.2. Cold-Season Emissions

The simulated  $\text{CH}_4$  fluxes show clear seasonality (Figure 1, for  $60^{\circ}$ – $90^{\circ}\text{N}$ ; Figure S2 in Supporting Information S1 for  $45^{\circ}$ – $90^{\circ}\text{N}$ ), with midsummer peaks that reflect higher temperatures, deeper soil thawing, enhanced vegetation activity, and wetland expansion under humid conditions. The simulated seasonal change, especially of the model-mean emissions, is consistent with the seasonal change in the eddy-covariance data upscaled with the machine learning model. As shown by Taylor diagrams (Taylor, 2001) for temporal variability, the simulated fluxes are strongly correlated with the upscaled flux (coefficient of determination  $R^2$  of  $>0.9$ ; Figure S3 in Supporting Information S1). However, the sixfold difference in peak  $\text{CH}_4$  emissions among the models, as shown by the standard deviations, is striking. Because prescribed climate and inundation data were used, this difference can be attributed to differences in the parameterizations and assumed sensitivity of the models. In the non-summer months, emissions simulated by most models were lower than the observations. Only  $0.7 \pm 1.8\%$  of the annual  $\text{CH}_4$  emissions simulated by the models occurred during the midwinter months (December–February) in  $60^{\circ}$ – $90^{\circ}\text{N}$  wetlands, whereas 8.3% of the upscaled flux occurred in those months (Table S3 in Supporting Information S1). The emissions simulated during non-summer months (September–May) and subzero air temperature months accounted for  $27 \pm 9\%$  ( $2.8 \pm 1.9 \text{ Tg CH}_4 \text{ yr}^{-1}$ ) and  $5.1 \pm 4.7\%$  ( $0.5 \pm 0.6 \text{ Tg CH}_4 \text{ yr}^{-1}$ ) of annual emissions; by comparison, in the upscaled flux data, the non-summer months account for 45% of annual emissions. Cold-season  $\text{CH}_4$  fluxes are difficult to evaluate with top-down approaches, but Tenkanen et al. (2021) recently used an atmospheric inversion system (CarbonTracker Europe) to estimate whole-year wetland fluxes. They estimated annual emissions from  $>50^{\circ}\text{N}$  wetlands to be  $23.1 \text{ Tg CH}_4 \text{ yr}^{-1}$ , of which 15% occurred in the cold-season (defined by satellite data by soil in the freeze/thaw state).

The contribution of cold-season emissions estimated by contemporary wetland models is notable but is still lower than that indicated by eddy covariance observations. This implies the necessity of model improvements not only in growing seasons but also in non-growing cold seasons. Simulated emissions in midwinter and subzero air



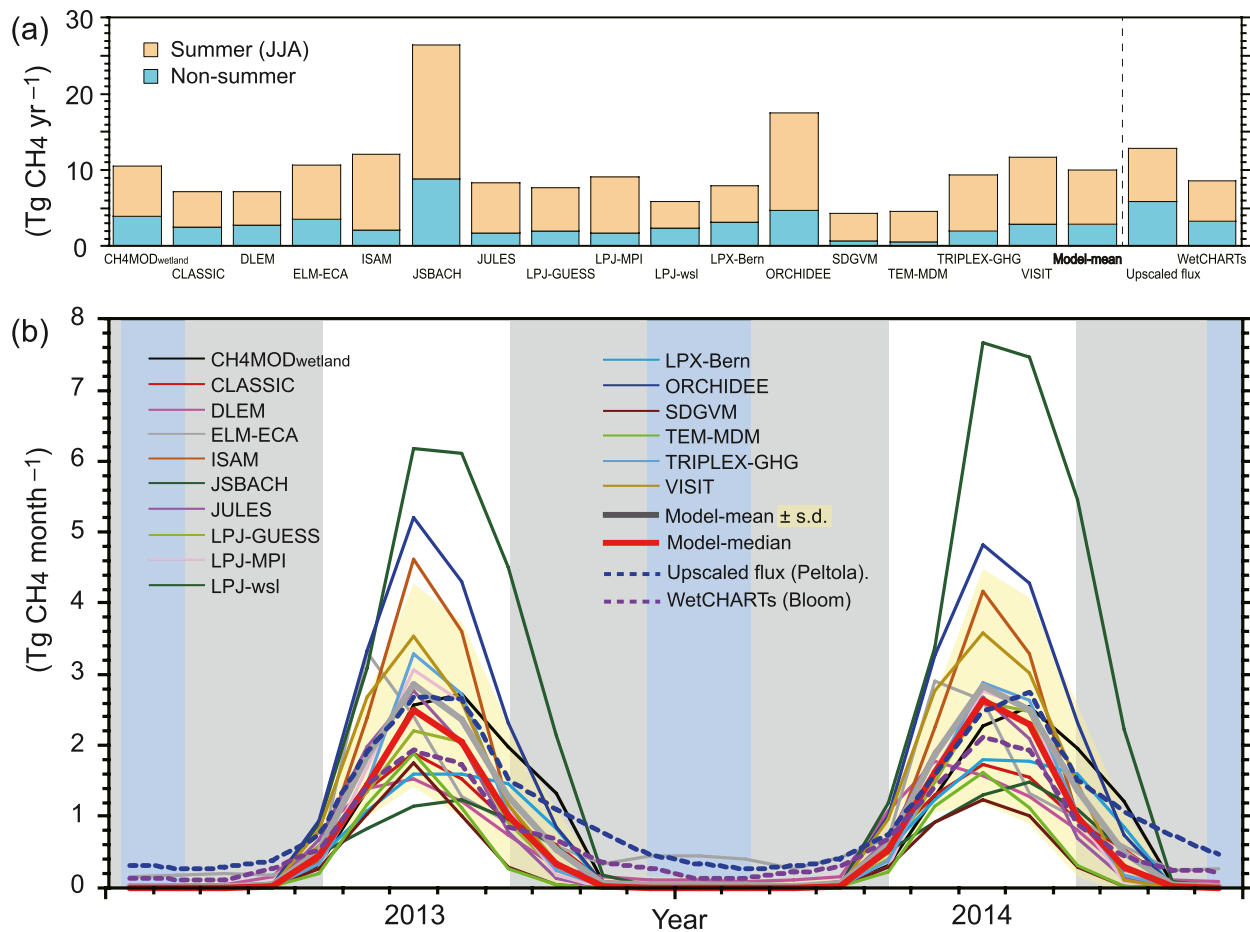


**Figure 1.** CH<sub>4</sub> fluxes from northern (>60°N) wetlands as simulated by each of the 16 models during 2013 and 2014. (a) Annual emissions during summer (June–August) and non-summer months and (b) monthly fluxes. The results were compared with eddy-covariance flux data upscaled with a machine learning model by Peltola et al. (2019) and data of an independent model study (WetCHARTs: Bloom et al., 2017). Light gray zones represent non-summer months (September–May), and pale blue zones represent midwinter months (December–February). See Figure S2 in Supporting Information S1 for the results for temperate to northern (>45°N) wetlands.

temperature periods were generally low, whereas those in autumn and spring were substantial. We found that the model-simulated CH<sub>4</sub> fluxes differed widely during the “zero-curtain” periods in spring and autumn, although their contributions to annual flux were comparable to that of the observation-based flux (3%–5% in spring and 8%–11% in autumn, Table S4 in Supporting Information S1). The stronger autumn emissions are consistent with those observed in Alaskan wetlands due soil physical conditions (Bao et al., 2021).

### 3.3. Spatial Distribution of Fluxes

Model-mean maps of simulated CH<sub>4</sub> fluxes show that substantial emissions occurred during the cold-season in the West Siberian and Hudson Bay Lowlands, along the western coast of North America, and in northern Europe (Figure 2; see Figure S4 in Supporting Information S1 for individual model results). In most northern wetlands, emissions during midwinter (December–February) were low, and their contribution to the total annual flux was less than 20%. Instead, substantial contributions in these months come from temperate wetlands of Europe, where winter conditions are less frigid. Emissions during the non-summer period (September–May) were substantial across a broad area of northern wetlands (Figure 2d) and their contributions to the annual flux were also notable, except in major wetlands that have high summer emissions. Soil freezing in autumn and thawing in spring were accompanied by large CH<sub>4</sub> emissions, but in major wetlands, these contributions were still comparatively low. Emissions during the subzero temperature period (which varied spatially among grids) were higher than those in midwinter and lower than those in non-summer months (Figure 2c). In Central and East Siberia, as well as in Europe, the simulated emissions during the subzero temperature period were substantial (>30%). The simulated

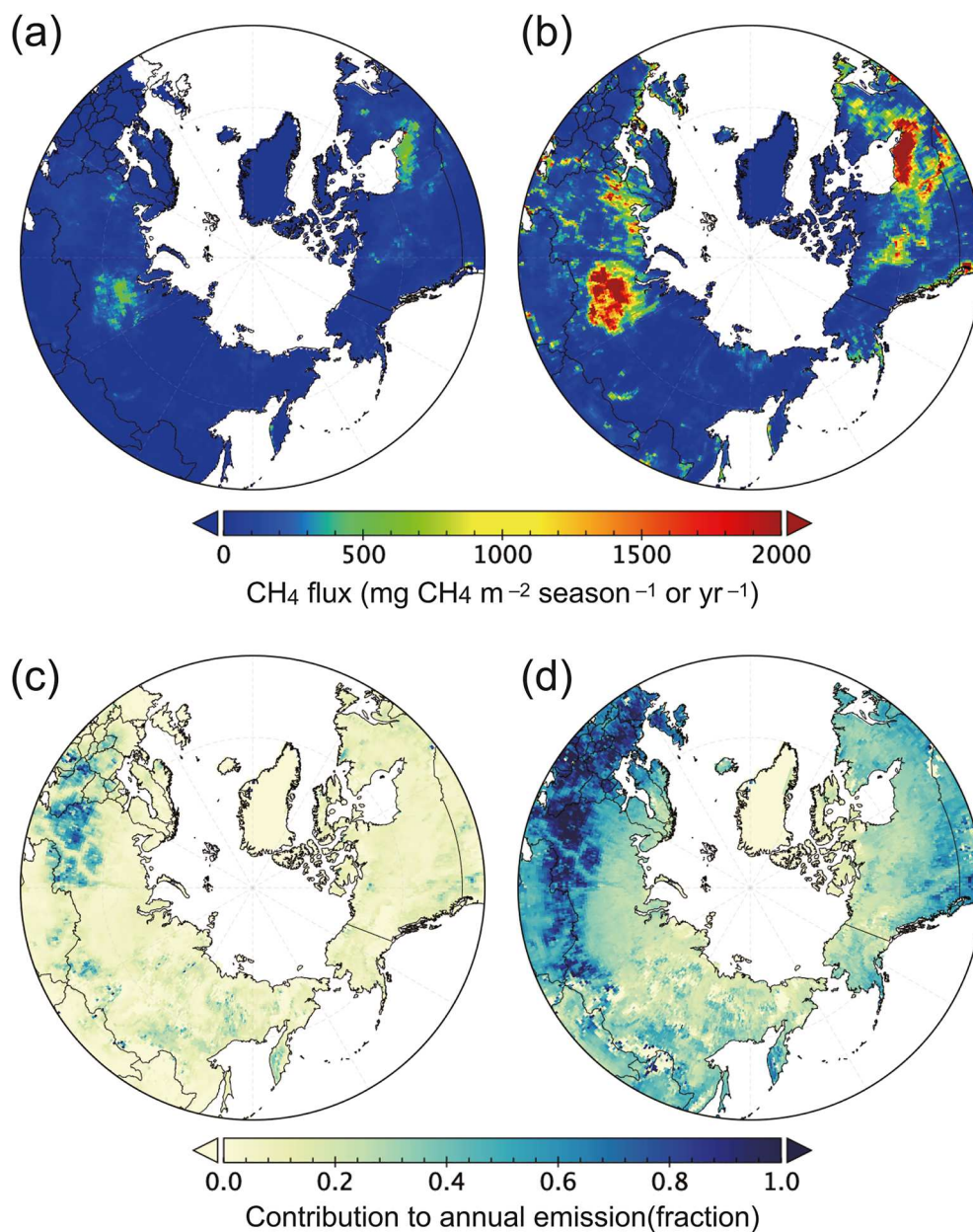


**Figure 2.** Model-composite maps of averaged CH<sub>4</sub> emissions during 2000–2020 simulated by 16 models. Mean fluxes during (a) subzero air temperature periods, (b) the non-summer season (September–May) and (c, d) contributions of (a) and (b), respectively, to the annual CH<sub>4</sub> budget (Figure S1 in Supporting Information S1). See Figure S4 in Supporting Information S1 for the results of each model.

cold-season emission patterns appear comparable to those of the upscaled flux data but differ in the magnitude of their contributions to annual flux (Figure S5 in Supporting Information S1). In the upscaled flux data, the contributions of emissions at subzero air temperatures were substantial in far East Siberia and Alaska, and non-summer emissions were substantial across a wide area of Central and East Siberia and northern North America.

We used dendrograms to identify clusters in the spatial patterns simulated by the different models and the upscaled observations (Figure S6 in Supporting Information S1). For non-summer emissions from >60°N wetlands, three small groups of models were identified: (a) CH<sub>4</sub>MODwetland and CLASSIC; (b) LPJ-wsl, LPX-Bern, and ORCHIDEE; and (c) ISAM, JULES, LPJ-GUESS, LPJ-MPI, SDGVM, TEM-MDM, TRIPLES-GHG, and VISIT. Several models (DLEM, JSBACH, and ELM-ECA) showed model-specific patterns. Similar (but not the

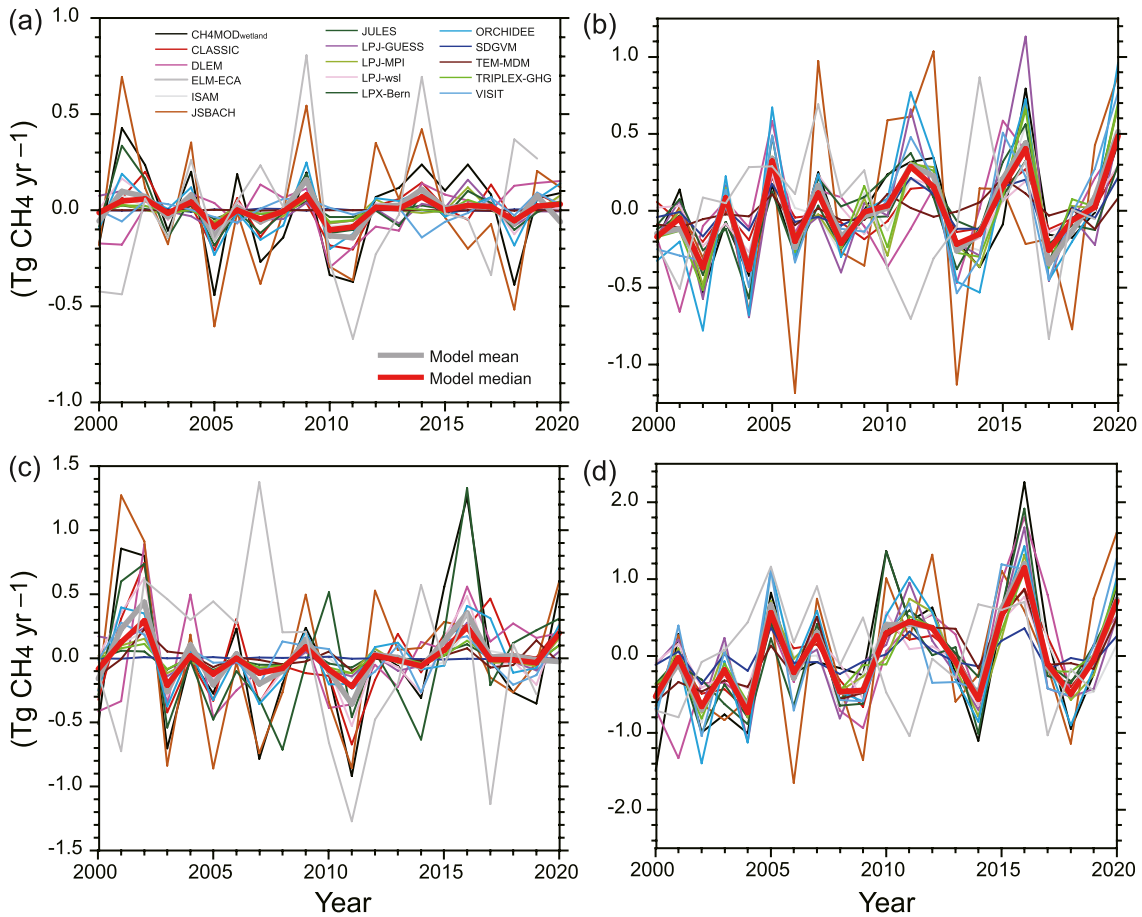


**Figure 3.** Interannual variability of wetland CH<sub>4</sub> fluxes for (a, b) >45°N and (c, d) >60°N simulated by 16 models, shown by deviations from the long-term mean, in (a, c) subzero air temperature months and (b, d) non-summer months (September–May).

same) clustering was found for emissions at subzero air temperatures and from >45°N wetlands. It looks that DLEM, which estimates CH<sub>4</sub> production from dissolved organic carbon, is relatively close to the reference data, although the model gave total cold-season emissions comparable to other models (Table S3 in Supporting Information S1). Apparently, results of the models adopting the same wetland schemes (e.g., ISAM and LPJ-GUESS implementing a scheme of Wania et al. (2010)) were close, but attributing the cluster formation to specific model attributes (Table S1 in Supporting Information S1) was, however, difficult, because they were related to many factors working at once.

### 3.4. Interannual Variability

This study first revealed that emissions during the cold periods showed substantial interannual variability (Figure 3), although previous studies focused on annual emissions dominated by growing-season emissions (e.g., Poulter et al., 2017; Thompson et al., 2017). Because variability of the simulated flux was caused mainly by inundation and temperature variabilities of the prescribed input data, most models showed coherent year-on-year variation. Higher non-summer emissions were simulated in 2005, 2011, 2016, and 2020, when the mean air temperature was higher than the long-term average (Figure 3a). As a result of interannual variability in emissions, the contribution of the cold-season to the annual flux also varied from  $18 \pm 9\%$  in 2002 to  $24 \pm 9\%$  in 2005 (16 model-mean). During the study period, the simulated flux increased gradually with time (on average,  $+0.4 \pm 0.8\%$  decade<sup>-1</sup>: from  $-0.004$  to  $+0.025$  Tg CH<sub>4</sub> yr<sup>-2</sup>, depending on the model). Rößger et al. (2022) have reported that, at one wet tundra site in Siberia, CH<sub>4</sub> emissions in June and July have been increasing substantially, and the results of the present study imply that cold-season emissions are also increasing, though long-term observation data supporting the trend are still insufficient (e.g., Masyagina & Menyailo, 2020). The simulated widths



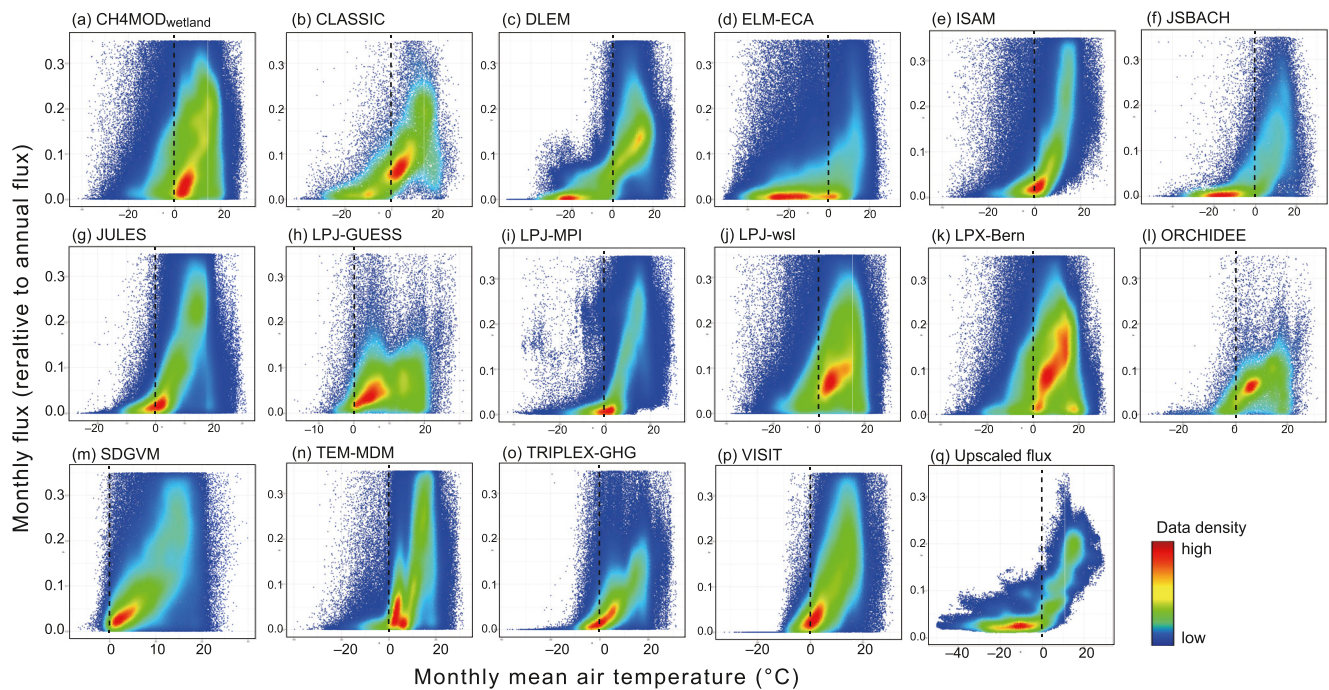


**Figure 4.** Relationship between monthly mean air temperature and monthly  $\text{CH}_4$  fluxes normalized by the annual total flux from northern ( $>45^\circ\text{N}$ ) wetlands simulated in each model grid. Color shows point density, from low (blue) to high (red). See Figure S7 in Supporting Information S1 for absolute fluxes (in  $\text{kg CH}_4 \text{ m}^{-2} \text{ month}^{-1}$ ).

of interannual variability of fluxes during the subzero air temperature period were smaller than those during the cold-season (Figure 3b), mainly by a methodological reason. Namely, because the length of the subzero temperature period varies inversely with average temperature (i.e., the subzero period is shorter in warm years), cumulative emissions during the subzero temperature period in individual years may be relatively stable when averaged over all models. As a result, interannual variability of the non-summer flux was strongly correlated ( $R^2 = 0.70$  for the model-mean) with the variability of annual emissions, while that of the subzero temperature period was correlated only poorly ( $R^2 = 0.04$ ).

### 3.5. Temperature Response Functions

The simulated relationship between temperature and the  $\text{CH}_4$  flux differed among the models; therefore, to compare results among the models, we standardized all fluxes by the annual flux (Figure 4, see Figure S7 in Supporting Information S1 for bulk fluxes). Several models showed an exponential relationship between flux rate and air temperature, reflecting their parameterizations (e.g., CLASSIC, ISAM, JULES, TRIPLEX-GHG, and VISIT). Several models estimated substantial  $\text{CH}_4$  emissions from subzero-temperature grid points (e.g., DLEM, ELM-ECA, and JSBACH), whereas a few models discretely suppressed emissions under subzero temperatures (e.g., LPJ-GUESS and SDGVM). Other models exhibited complicated patterns with multiple modes (e.g.,  $\text{CH4MOD}_{\text{wetland}}$ , DLEM, LPX-Bern, TEM-MDM). Differences in simulated fluxes under subzero temperatures may be attributable to model-specific parameterizations of biogeochemical factors such as the threshold temperature of microbial activity, the impact of vegetation activity, the spatial representativeness stemming from the data used, and the snow insulation effect (Table S1 in Supporting Information S1). For example, several models set a clear temperature threshold for  $\text{CH}_4$  production (e.g., LPJ-GUESS, TEM-MDM, TRIPLEX-GHG, and VISIT), whereas other models assume that production continues at subzero temperatures in parallel to heterotrophic respiration (e.g.,  $\text{CH4MOD}_{\text{wetland}}$ , CLASSIC, JSBACH, LPJ-MPI, and LPX-Bern).

Adjusting the simulated cold-season flux to better reproduce field evidence will result in higher winter and then annual simulated emissions (e.g., Treat et al., 2018) and increase the region's contribution more to the global  $\text{CH}_4$  budget. Although the models captured the seasonal cycle of emissions seen in observations, their quantitative accuracy was low, as revealed by the model intercomparison analyses. The models differed in the temperature responsiveness of emissions at temperatures around freezing, likely because of their different soil

structure and physical and biogeochemical parameterizations (Ueyama et al., 2023). For example, several models assumed threshold temperatures for CH<sub>4</sub> production and emission, but it should be examined against the observed temperature–flux relationships (Figure S8 and Text S1 in Supporting Information S1). Also, explicit soil-layer schemes are required to capture the processes during the zero-curtain periods, and observation-based tuning of key parameters such as temperature sensitivity of CH<sub>4</sub> production is required.

A revised parameterization specifically for capturing cold-season CH<sub>4</sub> emissions may be required, although it has been proposed that growing-period CH<sub>4</sub> production shows a consistent temperature dependence (Yvon-Durocher et al., 2014). Note that wetland models account also for methane oxidation in aerobic layers, which responds to temperature and affects local fluxes (e.g., Juutinen et al., 2022; Virkkala et al., 2023) but was differently parameterized in the models. Differences in the CH<sub>4</sub> transport pathways assumed in the models also partly account for the differences in fluxes at subzero temperatures. Diffusive emission likely dominates cold-season fluxes, but models differ in how gas diffusivity is treated in subzero-temperature soils as well as assumptions about other (i.e., plant-mediated and ebullition) pathways. Moreover, ice wedge and permafrost parameterizations, which were not examined in this study, would cause additional differences among the models. Masyagina and Menyailo (2020) showed that CH<sub>4</sub> emission characteristics differ between permafrost and non-permafrost areas in northern high latitudes, and Wickland et al. (2020) reported that ice wedge degradation enhances CH<sub>4</sub> emissions at landscape scale. Observations showed high heterogeneity of northern wetlands (e.g., ice wedge, polygon, hammock), which cannot be directly retrieved by broad-scale models, and therefore appropriate scaling schemes should be developed and introduced into wetland models. For model improvements and validation, our findings strongly encourage correcting year-round CH<sub>4</sub> flux data from more sites in high-latitude regions.

#### 4. Concluding Remarks

Global CH<sub>4</sub> budget would be more important in terms of climatic projection and mitigation (e.g., Kleinen et al., 2021; Zhang et al., 2017). Ongoing global warming, especially at high latitudes with Arctic amplification (Dai et al., 2019; Previdi et al., 2021) will increase the importance of CH<sub>4</sub> emissions from northern wetlands to the CH<sub>4</sub> budget. This study confirmed the importance of cold-season emissions as suggested by field observations, and further studies are needed to estimate the future CH<sub>4</sub> emissions. Future projection of wetland CH<sub>4</sub> budget would be more difficult by including direct human impacts such as land-use conversion (e.g., Qiu et al., 2021; Strack et al., 2019) and indirect impacts through changes in disturbance regimes accompanied with permafrost degradation (e.g., Miner et al., 2022). This study used outputs of the “diagnostic” experience in which inundation area was prescribed, and using of model-estimated inundation extent may introduce additional model specificities in hydrological dynamics. These aspects of wetland CH<sub>4</sub> models are being examined at global scales by comparing with atmospheric data (e.g., Chang et al., 2023), but specific analyses as done here are effective to specify important areas, periods, and processes.

#### Data Availability Statement

Datasets contributing to the Global Methane Budget by the GCP including wetland model estimates are archived in the International Carbon Observation System: <https://doi.org/10.18160/gcp-ch4-2019>. Tier one (CC-BY-4.0) FLUXNET-CH<sub>4</sub> data are available from <https://fluxnet.org/data/fluxnet-ch4-community-product/>. Upscaled flux data by Peltola et al. (2019) are available from: <https://doi.org/10.5281/zenodo.3247295>. WetCHARTs data are available from: <https://doi.org/10.3334/ORNLDAAC/1915>.

#### References

- Arndt, K. A., Oechel, W. C., Goodrich, J. P., Bailey, B. A., Kalhori, A., Hashemi, J., et al. (2019). Sensitivity of methane emissions to later soil freezing in Arctic tundra ecosystems. *Journal of Geophysical Research: Biogeosciences*, 124(8), 2595–2609. <https://doi.org/10.1029/2019JG005242>
- Arora, V. K., Melton, J. R., & Plummer, D. (2018). An assessment of natural methane fluxes simulated by the CLASS-CTEM model. *Biogeosciences*, 15, 4683–4809. <https://doi.org/10.5194/bg-15-4683-2018>
- Bao, T., Xu, X., Jia, G., Billesbach, D. P., & Sullivan, R. C. (2021). Much stronger tundra methane emissions during autumn freeze than spring thaw. *Global Change Biology*, 27(2), 376–387. <https://doi.org/10.1111/gcb.15421>
- Bartlett, K. B., & Harriss, R. C. (1993). Review and assessment of methane emissions from wetlands. *Chemosphere*, 26(1–4), 261–320. [https://doi.org/10.1016/0045-6535\(93\)90427-7](https://doi.org/10.1016/0045-6535(93)90427-7)

#### Acknowledgments

This study is a contribution to the global CH<sub>4</sub> synthesis organized by the Global Carbon Project, and all model simulations were conducted using the protocol and input data prepared by the project. AI was supported by the Environmental Research and Technology Development Fund (JPMEERF21S20830 and JPMEERF21S12007) of the Ministry of the Environment and the Environmental Restoration and Conservation Agency of Japan, and the Arctic Challenge for Sustainability II (JPMXD1420318865) of the Ministry of Education, Culture, Sports, Science and Technology, Japan. PH is grateful for support from a University of Birmingham Fellowship and BEAR computing facilities. FJ acknowledges support by the Swiss National Science Foundation (#200020\_200511). TK acknowledges support from the German Federal Ministry of Education and Research (BMBF) through the project PalMod, Grant 01LP1507B.

- Bloom, A. A., Bowman, K. W., Lee, M., Turner, A. J., Schroeder, R., Worden, J. R., et al. (2017). A global wetland methane missions and uncertainty dataset for atmospheric chemical transport models (WetCHARTs version 1.0). *Geoscientific Model Development*, 10(6), 2141–2156. <https://doi.org/10.5194/gmd-10-2141-2017>
- Bohn, T. J., Melton, J. R., Ito, A., Kleinen, T., Spahni, R., Stocker, B. D., et al. (2015). WETCHIMP-WSL: Intercomparison of wetland methane emissions over West Siberia. *Biogeosciences*, 12(11), 3321–3349. <https://doi.org/10.5194/bg-12-3321-2015>
- Bubier, J. L., & Moore, T. R. (1994). An ecological perspective on methane emissions from northern wetlands. *Trends in Ecology & Evolution*, 9(12), 460–464. [https://doi.org/10.1016/0169-5347\(94\)90309-3](https://doi.org/10.1016/0169-5347(94)90309-3)
- Chang, K.-Y., Riley, W. J., Collier, N., McNicol, G., Fluet-Chouinard, E., Knox, S. H., et al. (2023). Observational constraints reduce model spread but not uncertainty in global wetland methane emission estimates. *Global Change Biology*. <https://doi.org/10.1111/gcb.16755>
- Clark, D. B., Mercado, L. M., Sitch, S., Jones, C. D., Gedney, N., Best, M. J., et al. (2011). The Joint UK Land Environment Simulator (JULES), model description – Part 2: Carbon fluxes and vegetation dynamics. *Geoscientific Model Development*, 4(3), 701–722. <https://doi.org/10.5194/gmd-4-701-2011>
- Christensen, T. R. (1993). Methane emission from Arctic tundra. *Biogeochemistry*, 21(2), 117–139. <https://doi.org/10.1007/bf00000874>
- Dai, A., Luo, D., Song, M., & Liu, J. (2019). Arctic amplification is caused by sea-ice loss under increasing CO<sub>2</sub>. *Nature Communications*, 10(1), 121. <https://doi.org/10.1038/s41467-018-07954-9>
- Delwiche, K. B., Knox, S. H., Malhotra, A., Fluet-Chouinard, E., McNicol, G., Feron, S., et al. (2021). FLUXNET-CH<sub>4</sub>: A global, multi-ecosystem dataset and analysis of methane seasonality from freshwater wetlands. *Earth System Science Data*, 13(7), 3607–3689. <https://doi.org/10.5194/essd-13-3607-2021>
- Dlugokencky, E. J., Nisbet, E. G., Fisher, R., & Lowry, D. (2011). Global atmospheric methane: Budget, changes and dangers. *Philosophical Transactions of Royal Society of London*, A369(1943), 2058–2072. <https://doi.org/10.1098/rsta.2010.0341>
- Elberling, B., Nordström, C., Grøndahl, L., Søngaard, H., Friberg, T., Christensen, T. R., et al. (2008). High-arctic soil CO<sub>2</sub> and CH<sub>4</sub> production controlled by temperature, water, freezing and snow. *Advances in Ecological Research*, 40, 441–472. [https://doi.org/10.1016/S0065-2504\(07\)00019-0](https://doi.org/10.1016/S0065-2504(07)00019-0)
- Global Methane Pledge. (2021). Global methane pledge. Retrieved from <https://www.globalmethanepledge.org/>
- Harris, I., Osborn, T. J., Jones, P., & Lister, D. (2020). Version 4 of the CRU TS monthly high-resolution gridded multivariate climate dataset. *Scientific Data*, 7(1), 109. <https://doi.org/10.1038/s41597-020-0453-3>
- Howard, D., Agnan, Y., Helmig, D., Yang, Y., & Obrist, D. (2020). Environmental controls on ecosystem-scale cold-season methane and carbon dioxide fluxes in an Arctic tundra ecosystem. *Biogeosciences*, 17(15), 4025–4042. <https://doi.org/10.5194/bg-17-4025-2020>
- Hugelius, G., Strauss, J., Zubrzycki, S., Harden, J. W., Schuur, E. A. G., Ping, C. L., et al. (2014). Estimated stocks of circumpolar permafrost carbon with quantified uncertainty ranges and identified data gaps. *Biogeosciences*, 11(23), 6573–6593. <https://doi.org/10.5194/bg-11-6573-2014>
- Intergovernmental Panel on Climate Change (IPCC). (2021). *Climate change 2021: The physical science basis*. Cambridge University Press.
- Ito, A. (2019). Methane emission from pan-Arctic natural wetlands estimated using a process-based model, 1901–2016. *Polar Science*, 21, 26–36. <https://doi.org/10.1016/j.polar.2018.12.001>
- Ito, A., & Inatomi, M. (2012). Use of a process-based model for assessing the methane budgets of global terrestrial ecosystems and evaluation of uncertainty. *Biogeosciences*, 9(2), 759–773. <https://doi.org/10.5194/bg-9-759-2012>
- Jackson, R. B., Saunio, M., Bousquet, P., Canadell, J. G., Poulter, B., Stavert, A. R., et al. (2020). Increasing anthropogenic methane emissions arise equally from agriculture and fossil fuel sources. *Environmental Research Letters*, 15(7), 071002. <https://doi.org/10.1088/1748-9326/ab9ed2>
- Juutinen, S., Aurela, M., Tuovinen, J. P., Ivakhov, V., Linkosalmi, M., Räsänen, A., et al. (2022). Variation in CO<sub>2</sub> and CH<sub>4</sub> fluxes among land cover types in heterogeneous Arctic tundra in northeastern Siberia. *Biogeosciences*, 19(13), 3151–3167. <https://doi.org/10.5194/bg-19-3151-2022>
- Kleinen, T., Brovkin, V., & Schuldt, R. J. (2012). A dynamic model of wetland extent and peat accumulation: Results for the Holocene. *Biogeosciences*, 9(1), 235–248. <https://doi.org/10.5194/bg-9-235-2012>
- Kleinen, T., Gromov, S., Steil, B., & Brovkin, V. (2021). Atmospheric methane underestimated in future climate projections. *Environmental Research Letters*, 16(9), 094006. <https://doi.org/10.1088/1748-9326/ac1814>
- Kleinen, T., Mikolajewicz, U., & Brovkin, V. (2020). Terrestrial methane emissions from the Last Glacial Maximum to the preindustrial period. *Climate of the Past*, 16(2), 575–595. <https://doi.org/10.5194/cp-16-575-2020>
- Knox, S. H., Jackson, R. B., Poulter, B., McNicol, G., Fluet-Chouinard, E., Zhang, Z., et al. (2019). FLUXNET-CH<sub>4</sub> synthesis activity: Objectives, observations, and future directions. *Bulletin of the American Meteorological Society*, 100, 2608–2632. <https://doi.org/10.1175/BAMS-D-18-0268.1>
- Lehner, B., & Döll, P. (2004). Development and validation of a global database of lakes, reservoirs and wetlands. *Journal of Hydrology*, 296(1–4), 1–22. <https://doi.org/10.1016/j.jhydrol.2004.03.028>
- Le Mer, J., & Roger, P. (2001). Production, oxidation, emission and consumption of methane by soils: A review. *European Journal of Soil Biology*, 37(1), 25–50. [https://doi.org/10.1016/S1164-5563\(01\)01067-6](https://doi.org/10.1016/S1164-5563(01)01067-6)
- Li, T., Lu, Y., Yu, L., Sun, W., Zhang, Q., Zhang, W., et al. (2020). Evaluation of CH4MOD<sub>wetland</sub> and Terrestrial Ecosystem Model (TEM) used to estimate global CH<sub>4</sub> emissions from natural wetlands. *Geoscientific Model Development*, 13(8), 3769–3788. <https://doi.org/10.5194/gmd-13-3769-2020>
- Li, T., Raivonen, M., Alekseychik, P., Aurela, M., Lohila, A., Zheng, X., et al. (2016). Importance of vegetation classes in modeling CH<sub>4</sub> emissions from boreal and subarctic wetlands in Finland. *Science of the Total Environment*, 572, 1111–1122. <https://doi.org/10.1016/j.scitotenv.2016.08.020>
- Liu, L., Zhuang, Q., Oh, Y., Shurpali, N. J., Kim, S., & Poulter, B. (2020). Uncertainty quantification of global net methane emissions from terrestrial ecosystems using a mechanistically based biogeochemistry model. *Journal of Geophysical Research: Biogeosciences*, 125(6), e2019JG005428. <https://doi.org/10.1029/2019JG005428>
- Mastepanov, M., Sigsgaard, C., Dlugokencky, E. J., Houweling, S., Ström, L., Tamstorf, M. P., & Christensen, T. R. (2008). Large tundra methane burst during onset of freezing. *Nature*, 456(7222), 628–630. <https://doi.org/10.1038/nature07464>
- Masyagina, O. V., & Menyailo, O. V. (2020). The impact of permafrost on carbon dioxide and methane fluxes in Siberia: A meta-analysis. *Environmental Research*, 182, 109096. <https://doi.org/10.1016/j.envres.2019.109096>
- McGuire, A. D., Christensen, T. R., Hayes, D., Heroult, A., Euskirchen, E., Kimball, J. S., et al. (2012). An assessment of the carbon balance of Arctic tundra: Comparisons among observations, process models, and atmospheric inversions. *Biogeosciences*, 9(8), 3185–3204. <https://doi.org/10.5194/bg-9-3185-2012>



- Melton, J. R., Wania, R., Hodson, E. L., Poulter, B., Ringeval, B., Spahni, R., et al. (2013). Present state of global wetland extent and wetland methane modelling: Conclusions from a model inter-comparison project (WETCHIMP). *Biogeosciences*, *10*(2), 753–788. <https://doi.org/10.5194/bg-10-753-2013>
- Miner, K. R., Turetsky, M. R., Malina, E., Bartsch, A., Tamminen, J., McGuire, A. D., et al. (2022). Permafrost carbon emissions in a changing Arctic. *Nature Reviews Earth & Environment*, *3*(1), 55–67. <https://doi.org/10.1038/s43017-021-00230-3>
- Nisbet, E. G., Manning, M. R., Dlugokencky, E. J., Fisher, R. E., Lowry, D., Michel, S. E., et al. (2019). Very strong atmospheric methane growth in the 4 years 2014–2017: Implications for the Paris Agreement. *Global Biogeochemical Cycles*, *33*(3), 318–342. <https://doi.org/10.1029/2018GB006009>
- Olefeldt, D., Turetsky, M. R., Crill, P. M., & McGuire, A. D. (2013). Environmental and physical controls on northern terrestrial methane emissions across permafrost zones. *Global Change Biology*, *19*(2), 589–603. <https://doi.org/10.1111/gcb.12071>
- Pallandt, M. M. T. A., Kumar, J., Mauritz, M., Schuur, E. A. G., Virkkala, A.-M., Celis, G., et al. (2022). Representativeness assessment of the pan-Arctic eddy covariance site network and optimized future enhancements. *Biogeosciences*, *19*(3), 559–583. <https://doi.org/10.5194/bg-19-559-2022>
- Peltola, O., Vesala, T., Gao, Y., Rätty, O., Alekseychik, P., Aurela, M., et al. (2019). Monthly gridded data product of northern wetland methane emissions based on upscaling eddy covariance observations. *Earth System Science Data*, *11*(3), 1263–1289. <https://doi.org/10.5194/essd-11-1263-2019>
- Pirk, N., Tamstorf, M. P., Lund, M., Mastepanov, M., Pedersen, S. H., Mylius, M. R., et al. (2016). Snowpack fluxes of methane and carbon dioxide from high Arctic tundra. *Journal of Geophysical Research: Biogeosciences*, *121*(11), 2886–2900. <https://doi.org/10.1002/2016JG003486>
- Poulter, B., Bousquet, P., Canadell, J. G., Ciais, P., Peregou, A., Saunio, M., et al. (2017). Global wetland contribution to 2000–2012 atmospheric methane growth rate dynamics. *Environmental Research Letters*, *12*(9), 094013. <https://doi.org/10.1088/1748-9326/aa8391>
- Previdi, M., Smith, K. L., & Polvani, L. M. (2021). Arctic amplification of climate change: A review of underlying mechanisms. *Environmental Research Letters*, *16*(9), 093003. <https://doi.org/10.1088/1748-9326/ac1c29>
- Qiu, C., Ciais, P., Zhu, D., Guenet, B., Peng, S., Petrescu, A. M. R., et al. (2021). Large historical carbon emissions from cultivated northern peatlands. *Science Advances*, *7*(23), eabf1332. <https://doi.org/10.1126/sciadv.abf1332>
- Qu, Z., Jacob, D. J., Shen, L., Lu, X., Zhang, Y., Scarpelli, T. R., et al. (2021). Global distribution of methane emissions: A comparative inverse analysis of observations from the TROPOMI and GOSAT satellite instruments. *Atmospheric Chemistry and Physics*, *21*(18), 14159–14175. <https://doi.org/10.5194/acp-21-14159-2021>
- Rafat, A., Byun, E., Rezanezhad, F., Quinton, W. L., Humphreys, E. R., Webster, K., & Van Cappellen, P. (2022). The definition of the non-growing season matters: A case study of net ecosystem carbon exchange from a Canadian peatland. *Environmental Research Communications*, *4*(2), 021003. <https://doi.org/10.1088/2515-7620/ac53e2>
- Riley, W. J., Subin, Z. M., Lawrence, D. M., Swenson, S. C., Torn, M. S., Meng, L., et al. (2011). Barriers to predicting changes in global terrestrial methane fluxes: Analyses using CLM4Me, a methane biogeochemistry model integrated in CESM. *Biogeosciences*, *8*(7), 1925–1953. <https://doi.org/10.5194/bg-8-1925-2011>
- Ringeval, B., de Noblet-Ducoudré, N., Ciais, P., Bousquet, P., Prigent, C., Papa, F., & Rossow, W. B. (2010). An attempt to quantify the impact of changes in wetland extent on methane emissions on the seasonal and interannual time scales. *Global Biogeochemical Cycles*, *24*, GB2003. <https://doi.org/10.1029/2008GB003354>
- Rößger, N., Sachs, T., Wille, C., Boike, J., & Kutzbach, L. (2022). Seasonal increase of methane emissions linked to warming in Siberian tundra. *Nature Climate Change*, *12*(11), 1031–1036. <https://doi.org/10.1038/s41558-022-01512-4>
- Saunio, M., Stavert, A. R., Poulter, B., Bousquet, P., Canadell, J. G., Jackson, R. B., et al. (2020). The global methane budget 2000–2017. *Earth System Science Data*, *12*(3), 1561–1623. <https://doi.org/10.5194/essd-12-1561-2020>
- Shu, S., Jain, A. K., & Khesghi, H. S. (2020). Investigating wetland and nonwetland soil methane emission and sinks across the contiguous United States using a land surface model. *Global Biogeochemical Cycles*, *34*(7), e2019GB006251. <https://doi.org/10.1029/2019GB006251>
- Singarayer, J. S., Valdes, P. J., Friedlingstein, P., Nelson, S., & Beerling, D. J. (2011). Late Holocene methane rise caused by orbitally controlled increase in tropical sources. *Nature*, *470*(7332), 82–85. <https://doi.org/10.1038/nature09739>
- Spahni, R., Joos, F., Stocker, B. D., Steinacher, M., & Yu, Z. C. (2013). Transient simulations of the carbon and nitrogen dynamics in northern peatlands: From the Last Glacial Maximum to the 21st century. *Climate of the Past*, *9*(3), 1287–1308. <https://doi.org/10.5194/cp-9-1287-2013>
- Spahni, R., Wania, R., Neef, L., van Weele, M., Pison, I., Bousquet, P., et al. (2011). Constraining global methane emission and uptake by ecosystems. *Biogeosciences*, *8*(6), 1643–1665. <https://doi.org/10.5194/bg-8-1643-2011>
- Strack, M., Hayne, S., Lovitt, J., McDermid, G. J., Rahman, M. M., Saraswati, S., & Xu, B. (2019). Petroleum exploration increases methane emissions from northern peatlands. *Nature Communications*, *10*(1), 2804. <https://doi.org/10.1038/s41467-019-10762-4>
- Taylor, K. E. (2001). Summarizing multiple aspects of model performance in a single diagram. *Journal of Geophysical Research*, *106*(D7), 7183–7192. <https://doi.org/10.1029/2000jd900719>
- Tenkanen, M., Aki, T., Rautiainen, K., Kangasaho, V., Ellul, R., & Aalto, T. (2021). Utilizing Earth observations of soil freeze/thaw data and atmospheric concentration to estimate cold season methane emissions in the northern high latitudes. *Remote Sensing*, *13*(24), 5059. <https://doi.org/10.3390/rs13245059>
- Thompson, R. L., Sasakawa, M., Machida, T., Aalto, T., Worthy, D., Lavric, J. T., et al. (2017). Methane fluxes in the high northern latitudes for 2005–2013 estimated using a Bayesian atmospheric inversion. *Atmospheric Chemistry and Physics*, *17*(5), 3553–3572. <https://doi.org/10.5194/acp-17-3553-2017>
- Tian, H., Xu, X., Liu, M., Ren, W., Zhang, C., Chen, G., & Lu, C. (2010). Spatial and temporal patterns of CH<sub>4</sub> and N<sub>2</sub>O fluxes in terrestrial ecosystems of North America during 1979–2008: Application of a global biogeochemistry model. *Biogeosciences*, *7*(9), 2673–2694. <https://doi.org/10.5194/bg-7-2673-2010>
- Treat, C. C., Bloom, A. A., & Marushchak, M. E. (2018). Nongrowing season methane emissions – A significant component of annual emissions across northern ecosystems. *Global Change Biology*, *24*(8), 3331–3343. <https://doi.org/10.1111/gcb.14137>
- Ueyama, M., Knox, S. H., Delwiche, K. B., Bansal, S., Riley, W. J., Baldocechi, D., et al. (2023). Modeled production, oxidation, and transport processes of wetland methane emissions in temperate, boreal, and Arctic regions. *Global Change Biology*, *10*(8), 2313–2334. <https://doi.org/10.1111/gcb.16594>
- Virkkala, A.-M., Niittynen, P., Kempainen, J., Marushchak, M. E., Voigt, C., Hensgens, G., et al. (2023). High-resolution spatial patterns and drivers of terrestrial ecosystem carbon dioxide, methane, and nitrous oxide fluxes in the tundra. *Biogeosciences Discussions*. <https://doi.org/10.5194/bg-2023-61>
- Wania, R., Ross, I., & Prentice, I. C. (2010). Implementation and evaluation of a new methane model within a dynamic global vegetation model: LPJ-WHyMe v1.3.1. *Geoscientific Model Development*, *3*(2), 565–584. <https://doi.org/10.5194/gmd-3-565-2010>

- Wickland, K. P., Jorgensen, M. T., Koch, J. C., Kanevskiy, M., & Striegl, R. G. (2020). Carbon dioxide and methane flux in a dynamic arctic tundra landscape: Decadal-scale impacts of ice wedge degradation and stabilization. *Geophysical Research Letters*, *47*, e2020GL089894. <https://doi.org/10.1029/2020GL089894>
- Xu, X., Riley, W. J., Koven, C. D., Billesbach, D. P., Chang, R. Y. W., Commann, R., et al. (2016). A multi-scale comparison of modeled and observed seasonal methane emissions in northern wetlands. *Biogeosciences*, *13*(17), 5043–5056. <https://doi.org/10.5194/bg-13-5043-2016>
- Yvon-Durocher, G., Allen, A. P., Bastviken, D., Conrad, R., Gudas, C., St-Pierre, A., et al. (2014). Methane fluxes show consistent temperature dependence across microbial to ecosystem scales. *Nature*, *507*(7493), 488–491. <https://doi.org/10.1038/nature13164>
- Zhang, Z., Fluet-Chouinard, E., Jensen, K., McDonald, K., Hugelius, G., Gumbrecht, T., et al. (2021). Development of the global dataset of wetland area and dynamics for methane modeling (WAD2M). *Earth System Science Data*, *13*(5), 2001–2023. <https://doi.org/10.5194/essd-13-2001-2021>
- Zhang, Z., Zimmermann, N. E., Kaplan, J. O., & Poulter, B. (2016). Modeling spatiotemporal dynamics of global wetlands: Comprehensive evaluation of a new sub-grid TOPMODEL parameterization and uncertainties. *Biogeosciences*, *13*(5), 1387–1408. <https://doi.org/10.5194/bg-13-1387-2016>
- Zhang, Z., Zimmermann, N. E., Stenke, A., Li, X., Hodson, E. L., Zhu, G., et al. (2017). Emerging role of wetland methane emissions in driving 21st century climate change. *Proceedings of the National Academy of Sciences of the United States of America*, *114*(36), 9647–9652. <https://doi.org/10.1073/pnas.1618765114>
- Zhu, Q., Liu, J., Peng, C., Chen, H., Fang, X., Jiang, H., et al. (2014). Modelling methane emissions from natural wetlands by development and application of the TRIPLEX-GHG model. *Geoscientific Model Development*, *7*(3), 981–999. <https://doi.org/10.5194/gmd-7-981-2014>
- Zona, D., Gioli, B., Commann, R., Landaas, J., Wofsy, S. C., Miller, C. E., et al. (2016). Cold season emissions dominate the Arctic tundra methane budget. *Proceedings of the National Academy of Sciences of the United States of America*, *113*(1), 40–45. <https://doi.org/10.1073/pnas.1516017113>

## References From the Supporting Information

- Chang, K. Y., Riley, W. J., Knox, S. H., Jackson, R. B., McNicol, G., Poulter, B., et al. (2021). Substantial hysteresis in emergent temperature sensitivity of global wetland CH<sub>4</sub> emissions. *Nature Communications*, *12*(1), 2266. <https://doi.org/10.1038/s41467-021-22452-1>
- Tian, H., Chen, G., Lu, C., Xu, X., Ren, W., Zhang, B., et al. (2015). Global methane and nitrous oxide emissions from terrestrial ecosystems due to multiple environmental changes. *Ecosystem Health and Sustainability*, *1*, 4–20. <https://doi.org/10.1890/EHS14-0015.1>
- Walter, B. P., & Heimann, M. (2000). A process-based, climate-sensitive model to derive methane emissions from natural wetlands: Application to five wetlands sites, sensitivity to model parameters, and climate. *Global Biogeochemical Cycles*, *14*(3), 745–765. <https://doi.org/10.1029/1999gb001204>
- Walter, B. P., Heimann, M., & Matthews, E. (2001). Modeling modern methane emissions from natural wetlands I. Model description and results. *Journal of Geophysical Research*, *106*(D24), 34189–34206. <https://doi.org/10.1029/2001jd900165>
- Wania, R., Ross, I., & Prentice, I. C. (2009). Integrating peatlands and permafrost into a dynamic global vegetation model: 1. Evaluation and sensitivity of physical land surface processes. *Global Biogeochemical Cycles*, *23*(3), GB3014. <https://doi.org/10.1029/2008GB003412>